SERI/TP-34-246R
UC CATEGORY: UC-62

INCIDENCE ANGLE MODIFIER AND AVERAGE OPTICAL EFFICIENCY OF PARABOLIC TROUGH COLLECTORS

H. GAUL
A. RABL

JULY 1979

PRESENTED AT THE 1979 SILVER JUBILEE INTERNATIONAL CONGRESS OF THE INTERNATIONAL SOLAR ENERGY SOCIETY IN JOINT MEETING WITH THE AMERICAN SECTION OF THE INTERNATIONAL SOLAR ENERGY SOCIETY, INC.
MAY 28 - JUNE 1, 1979; ATLANTA, GEORGIA

Solar Energy Research Institute

1536 Cole Boulevard
Golden, Colorado 80401

A Division of Midwest Research Institute

Prepared for the
U.S. Department of Energy
Contract No. EG-77-C-01-4042

Printed in the United States of America
Available from:
National Technical Information Service
U.S. Department of Commerce
5285 Port Royal Road
Springfield, VA 22161
Price:
Microfiche $3.00
Printed Copy $4.00

INCIDENCE ANGLE MODIFIER AND AVERAGE OPTICAL EFFICIENCY OF PARABOLIC TROUGH COLLECTORS

H. Gaul
A. Rabl
Solar Energy Research Institute
1536 Cole Boulevard
Golden, Colorado
80401 USA

ABSTRACT

The incidence angle modifier for parabolic troughs is investigated in order to clarify the connection between collector tests and prediction of long term energy delivery by collector arrays. The optical efficiency of a parabolic trough collector decreases with incidence angle for several reasons:

- decreased transmission and absorption,
- increased width of solar image on receiver, and
- spillover of radiation in troughs of finite length without end reflectors.

In order to be able to apply test results from a (usually short) collector module to collector arrays of arbitrary length, it is necessary to separate analytically the end loss from the first two effects. This analysis is applied to several collectors which have been tested at Sandia Laboratories and at the Solar Energy Research Institute (SERI). For improved accuracy, the measurements of the incidence angle modifier at SERI were carried out at low temperature with an open water test loop. The results are presented in two forms, first as a polynomial fit to the data, and second as a single number, the all-day average optical efficiency for typical operating conditions.

1. INTRODUCTION

Efficiency curves of solar collectors are usually measured and reported at normal or nearly normal incidence, which is the most reasonable choice for standardized test conditions. In actual operation, on the other hand, the incidence angle on any collector with less than full two-axis tracking varies over the course of the day and the year. In most collectors the efficiency varies with incidence angle and one must take this variation into account to predict correctly long term energy delivery (1-4). While this necessity is well recognized in the flat-plate literature, it has not received sufficient attention with regard to concentrators. This paper addresses this question in order to help formulate a standardized collector test procedure and to supply a missing piece of information for system analysis.

Since to an excellent approximation the optical and thermal properties of a solar collector can be considered to be independent of each other, the incidence angle affects only the optical efficiency η_o, i.e., the efficiency at ambient temperature. This paper discusses the measurement of the incidence angle modifier K, defined as

$$K(\theta) = \frac{\eta_o(\theta)}{\eta_o(\theta = 0)},$$

and shows how this factor must be combined with an end-loss factor to account for spilling of radiation over the end in line focus collectors of finite length. The method is illustrated with test results for parabolic troughs that have been obtained at Sandia Laboratories (5) and SERI. The results are presented in two forms: as curve fit of K versus θ, and as all-day average $\bar{K}$.

2. COLLECTOR PARAMETERS AND TEST PROCEDURE

The efficiency of solar thermal collectors usually is measured by flowing a heat transfer fluid through the collector and monitoring T_{in} and T_{out}. In terms of the mean fluid temperature

$$T_f = (T_{in} + T_{out})/2, \qquad [2\text{-}1]$$

the efficiency is

$$\eta = F'(\eta_o - U\Delta T/I), \qquad [2\text{-}2]$$

where

$$\Delta T = T_f - T_{ambient} \qquad [2\text{-}3]$$

and I = insolation per aperture area (for a line focus collector, $I = I_b \cos\theta$, where θ is the incidence angle and I_b is the beam irradiance as measured with a pyrheliometer). F' is a factor which accounts for the difference between fluid and absorber

surface temperature, η_o is the optical efficiency, and U is the heat loss coefficient (6,7). The fact that only the products $(F'\eta_o)$ and $(F'U)$ are measured is of no concern for this paper because F' is independent of θ. At nonzero incidence the optical efficiency decreases for several reasons:

- decreased transmission and absorption,
- increased width of solar image on receiver (8), and
- spillover of radiation in collectors of finite length without end reflectors.

In order to be able to apply test results from a (usually short) collector module to collector arrays of arbitrary length, it is necessary to separate analytically the end loss from the first two effects. This is accomplished by writing the efficiency equation in the form

$$\eta(\theta) = F'\left(\eta_o(\theta = 0)\, K(\theta)\Gamma(\theta) - U\Delta T/I\right), \quad [2\text{-}4]$$

where

$$K(\theta) = \frac{\eta_o(\theta)}{\eta_o(\theta = 0)}\bigg|_{\ell = \infty} \quad [2\text{-}5]$$

is the incidence angle modifier for infinitely long troughs. The end loss factor $\Gamma(\theta)$ is a strictly geometric quantity, defined as one minus the fraction of the rays incident on the aperture which spill over the end of a receiver of finite length. A straightforward, although slightly tedious, calculation yields the result

$$\Gamma(\theta) = 1 - \frac{f}{\ell}\left(1 + w^2/48f^2\right) \tan\theta \quad [2\text{-}6]$$

for a parabolic trough of length ℓ, aperture width w, and focal length f, assumming that the receiver has the same length ℓ and is placed symmetrically. If the receiver exceeds ℓ by an amount r on one side, Γ is modified to

$$\Gamma(\theta) = \min \begin{cases} 1 \\ 1 + \frac{r}{\ell} - \frac{f}{\ell}\left(1 + w^2/48f^2\right)\tan\theta \end{cases} \quad [2\text{-}7]$$

for the corresponding sign of θ. For example, if the receiver has an overhang r on the east side and no overhang on the west side, one must use Eq. [2-6] for negative θ (morning) and Eq. [2-7] for positive θ (afternoon).

Since the incidence angle affects only the optical term in Eq. [2-4], it is best to measure $\eta(\theta)$ at or near ambient temperature to minimize the heat loss correction. If this is not possible, the heat loss term $F'U\Delta T/I$ must be added to $\eta(\theta)$ to isolate the optical term $F'\eta_o(\theta = 0)\, K(\theta)\, \Gamma(\theta)$. If, as is the case in most collector test facilities, η is found by measuring flow rate and temperature rise $T_{out} - T_{in}$ across the collector, it is crucial that both T_{out} and T_{in} be stable. This requirement may be difficult to satisfy in a closed loop system because the solar energy input gradually raises the temperature of the fluid. Even if $T_{out} - T_{in}$ is stable under such conditions, it does not yield the true efficiency because T_{out} and T_{in}, measured simultaneously, do not correspond to the temperature increase of the same fluid element on its passage through the collector. In most cases this effect is more serious than the time constant of the collector itself.

While it is possible to apply appropriate corrections to closed loop measurements, we found it much simpler to carry out the tests at SERI with an open loop. Water from the water mains had sufficiently constant temperature for this purpose and could be discarded after passage through the collector. Water also has the advantage of a precisely known heat capacity.

If closed loop operation is desirable, one can still obtain accurate incidence angle results by resorting to the calorimetric method, i.e., by monitoring the temperature rise in a well mixed storage tank rather than $T_{out} - T_{in}$. Of course, a correction must then be applied for heat losses from tank and heat fluid transfer lines. (The correction factor is measured by observing the temperature drop when no collector is in the system.)

3. AVAILABLE DATA

3.1 Sandia Data

All-day performance curves have been obtained for several line focus collectors at the Collector Module Test Facility of Sandia Labs. (5). The parameters for these collectors are listed in Table 3-1. The optical and heat loss parameters $(F'\eta_o)$ and $(F'U)$ were derived by straight line interpolation of the instantaneous efficiency data. U is expected to increase with temperature, but the data points did not deviate sufficiently (i.e., compared to their accuracy) from a straight line to justify a second order fit. Also, any errors in long term performance predictions resulting from this approximation are very small, provided the same η_o and U are used consistently throughout.

A typical all-day performance curve from Ref. 5 is reproduced in Fig. 3-1. By itself such a curve applies only to the specific conditions at the time of the test. If one wants to know the energy delivery of this collector under different operating conditions (e.g., different tracking mode, different time of year, different temperature), one must calculate the incidence angle modifiers by the procedure described in Section 2. First, the time of day is converted to

Table 3-1. Collector Parameters for One-Module Parabolic Troughs[a]

Collector Type	$F'\eta_o$	F'U (W/m^2 °C)	Focal Length f (m)	Aperture Width w (m)	Aperture Length ℓ (m)	Rim Angle (degrees)	Geometric Concentration Ratio C [d]
Del	0.672	0.777[b]	0.107	0.610	2.440	110	10.2
Acurex	0.597	0.710	0.489	1.829	3.048	90	18.3
Solar Kinetics	0.666	0.695	0.267	1.040	6.100	90	13.0
Hexcel, Sandia	0.709	0.514	0.927	2.711	5.968	72	e
Hexcel, SERI	0.684	1.570	0.927	2.711	5.968	72	21.9[c]

[a]Receiver tube length was equal to aperture length except for Sandia version of Hexcel which had the receiver extending r = 30 cm beyond aperture on east side.
[b]η vs. $\Delta T/I$ curve not linear for Del collector; F'U given at 200°C average fluid temperature.
[c]Hexcel, SERI had no cover glazing or insulation at the receiver.
[d]The geometric concentration ratio C is defined as aperture area/receiver area; i.e., C = $w/\pi d$, where d = absorber tube diameter.
[e]Hexcel Sandia had radiation shield in back of receiver tube.

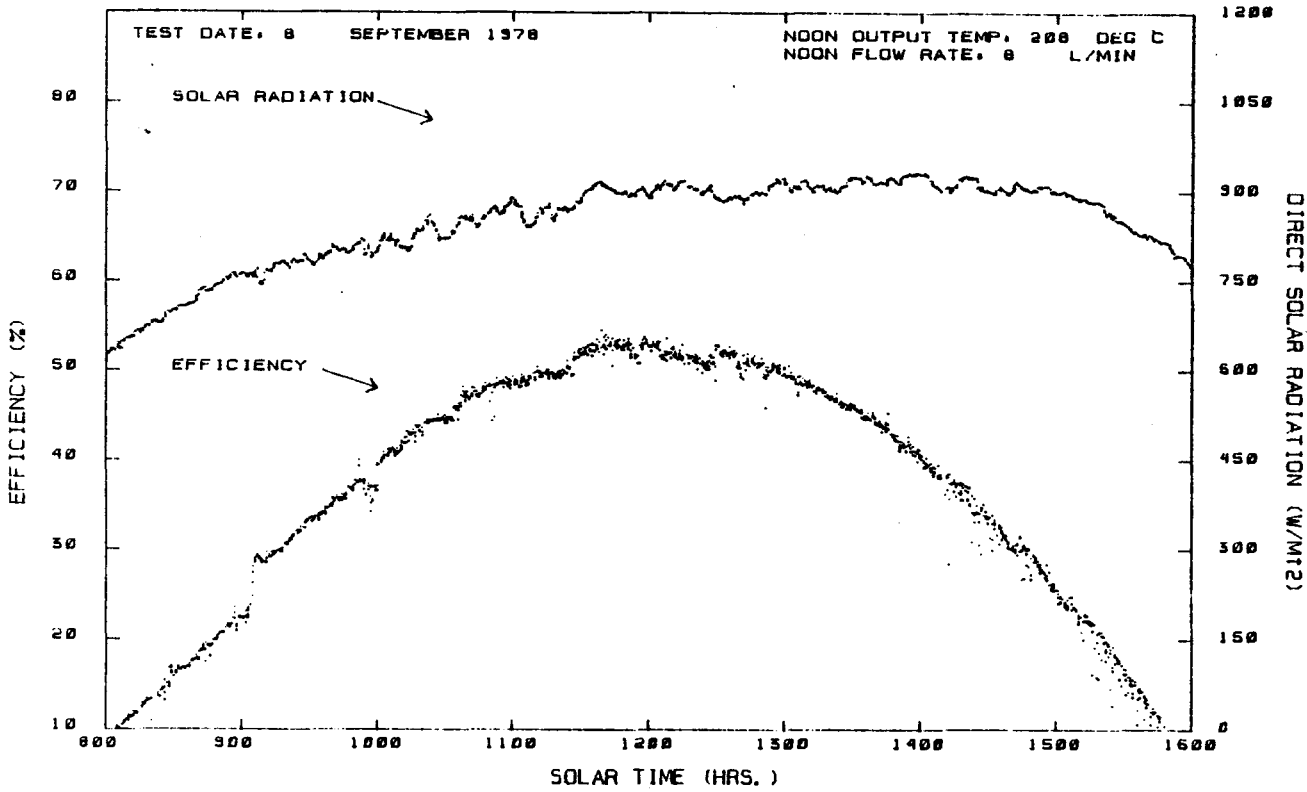

Fig. 3-1. Typical All-Day Efficiency Curve For Parabolic Trough as Measured by Sandia Laboratories. The definition of efficiency used by Sandia differs from ours by a factor of cos θ.

incidence angle by using the equation of time for the test day. Then $K(\theta)$ is extracted from Eq. [2-4] after inserting the relevant collector parameters from Table 3-1. The results, plotted in Fig. 4-1, are discussed in the following section.

Unfortunately, the accuracy of the Sandia all-day curves was severely limited by the fact that they were obtained by the flow rate method in a closed test loop that took several hours to reach equilibrium (9). To some extent the uncertainties caused by changing loop temperatures can be reduced by combining morning and afternoon data, as we have done wherever possible. In cases where clouds or tracking errors caused irregular drops in efficiency, we interpolated the data. When several all-day curves were available for the same collector, we averaged the incidence angle modifier to improve the accuracy. In view of the test procedure used, the uncertainty in the results may be large and difficult to estimate.

3.2 SERI Data

The Hexcel parabolic trough collector was shipped to SERI after testing at Sandia. This collector was tested in an open water loop at SERI in order to investigate its optical properties more thoroughly. The low temperature tests had the following goals:

- to determine the incidence angle modifier,
- to determine the optical errors of the collector (by measuring its performance as a function of misalignment angle, as described in Ref. 10), and
- to study effects of circumsolar radiation (to be described in a future report).

The receiver enclosure (glazing and heat shield described in Ref. 5) was removed for these tests in order to complement the Sandia measurements by testing a version of the collector that may be more promising for applications at lower temperatures for which improvement in η_o outweighs the increase in U. Also, the absorber tube was replaced since the original one had been damaged in transit.

The data for the incidence angle modifier were measured so close to ambient temperature that heat loss corrections amounted to a few percent at most. Also, these tests were carried out on days with little or no wind, hence uncertainties due to wind speed fluctuations were negligible.

4. RESULTS

The results of the analysis are shown in Fig. 4-1 as a plot of $K(\theta)$ versus incidence angle θ. Remarkably good straight line fits are obtained when $K(\theta)$ for flat-plate collectors is plotted against the variable $1/\cos\theta - 1$ (4), but, as shown in Fig. 4-2, $1/\cos\theta - 1$ is not a useful variable for parabolic trough collectors; the data points consistently curve downward at large angles. This feature is not surprising since in parabolic troughs a decrease of the intercept factor γ is superimposed on the decrease of the reflectance-absorptance product, and the functional dependence of these quantities is different (8). Theoretical calculation of $K(\theta)$ requires knowledge of the optical errors of the collector, and the functional dependence of α, ρ, and τ on θ; lacking this information, we have not attempted such a calculation.

In any case, for practical applications, only a curve fit to the data is needed, and a polynomial in θ with two adjustable parameters gives excellent fits. In choosing the coefficients we impose the constraints

$$K(\theta = 0) = 1 \qquad [4\text{-}1]$$

and

$$K\left(\theta = \frac{\pi}{2}\right) = 0. \qquad [4\text{-}2]$$

A linear term is unnecessary because the slope of K is practically zero at small angles. Therefore, we use the fit

$$K(\theta) = 1 + A\theta^2 + B\theta^3 + C\theta^4, \qquad [4\text{-}3]$$

subject to the constraint

$$1 + A\left(\frac{\pi}{2}\right)^2 + B\left(\frac{\pi}{2}\right)^3 + C\left(\frac{\pi}{2}\right)^4 = 0. \qquad [4\text{-}4]$$

The coefficients are determined by the method of least squares. The closeness between

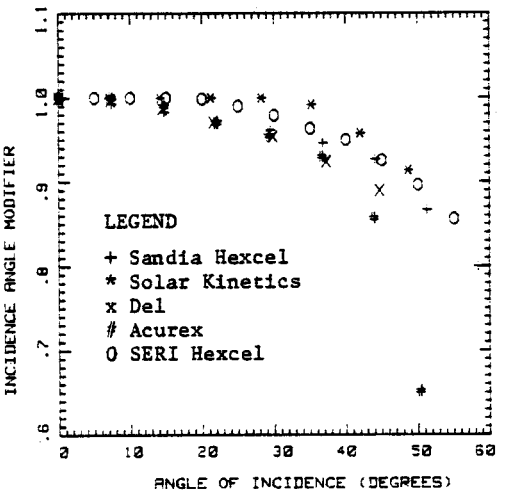

Fig. 4-1. Test Results for the Incidence Angle Modifier.

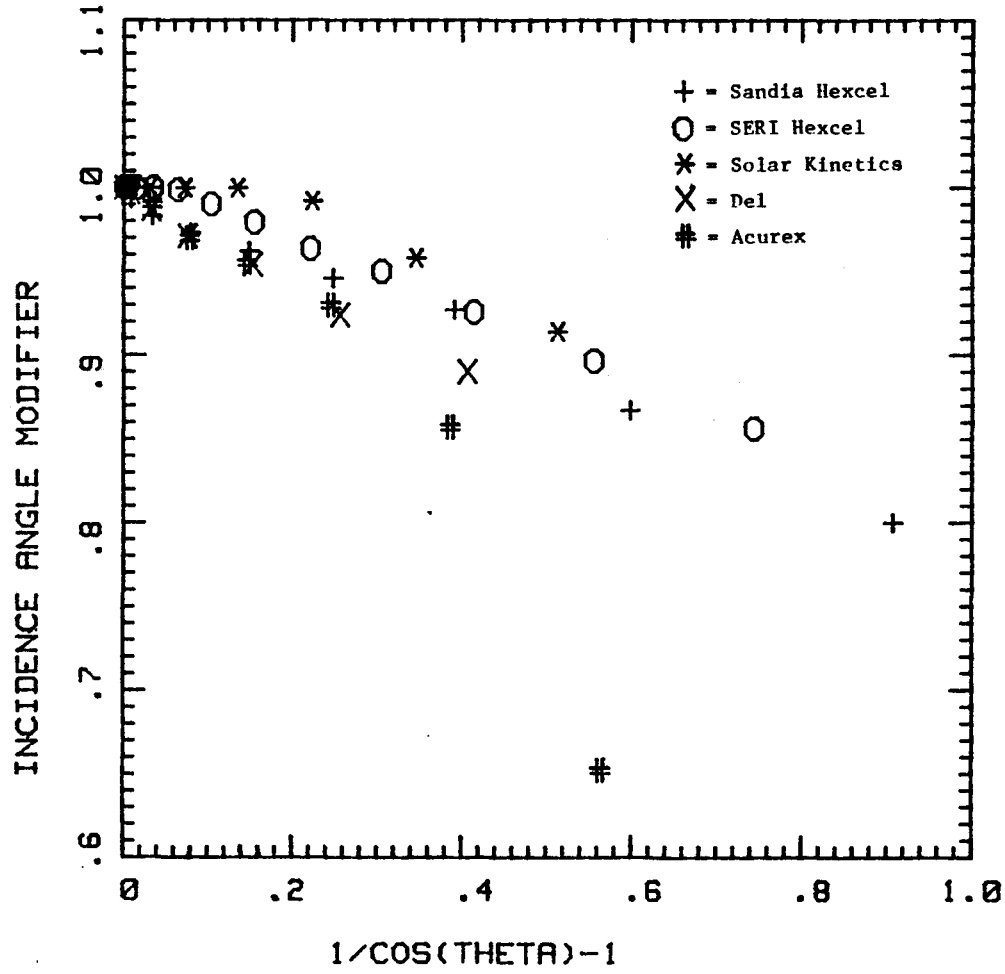

Fig. 4-2. Incidence Angle Modifier Plotted vs. 1/cos θ-1.

the data points and these fits is displayed in Fig. 4-3, and the numerical values of the coefficients are included.

5. ALL-DAY AVERAGE

For short-hand performance prediction methods (11,12), use of a single number, the all-day average optical efficiency $\bar{\eta}_o$, is far more convenient than the function $\eta_o(\theta)$. To be consistent with the utilizability method, the all-day average must be calculated with the beam irradiance I_b as a weighting factor. For this purpose the long term average meteorological correlations of the Liu and Jordan type (12) are appropriate; this is explained in the Appendix of Ref. 8. The beam irradiance corresponding to hour angle ω and sunset hour angle ω_s is given by the equation

$$I_b(\omega, \omega_s) = \left(a + b \cos \omega - \frac{H_d}{H_h}\right) K_h I_o, \quad [5\text{-}1]$$

where

$$a = 0.409 + 0.5016 \sin (\omega_s - 1.047), \quad [5\text{-}2]$$

$$b = 0.6609 - 0.4767 \sin (\omega_s - 1.047), \quad [5\text{-}3]$$

I_o = solar constant,

K_h = clearness index (ratio of terrestrial over extraterrestrial daily total irradiation on the horizontal surface), and

$\frac{H_d}{H_h}$ = ratio of diffuse over hemispherical daily total irradiation on the horizontal surface.

Since concentrating collectors operate primarily during sunny periods, one can assume $H_d/H_h = 0.23$ and $K_h = 0.75$ (the values of K_h and I_o do not matter for the calculations in this paper).

The all-day average is defined by the formula

$$\bar{y} = \frac{\int_0^{\omega_c} d\omega\, I_b(\omega) \cos\theta\, y(\theta)}{\int_0^{\omega_c} d\omega\, I_b(\omega) \cos\theta} \quad [5\text{-}4]$$

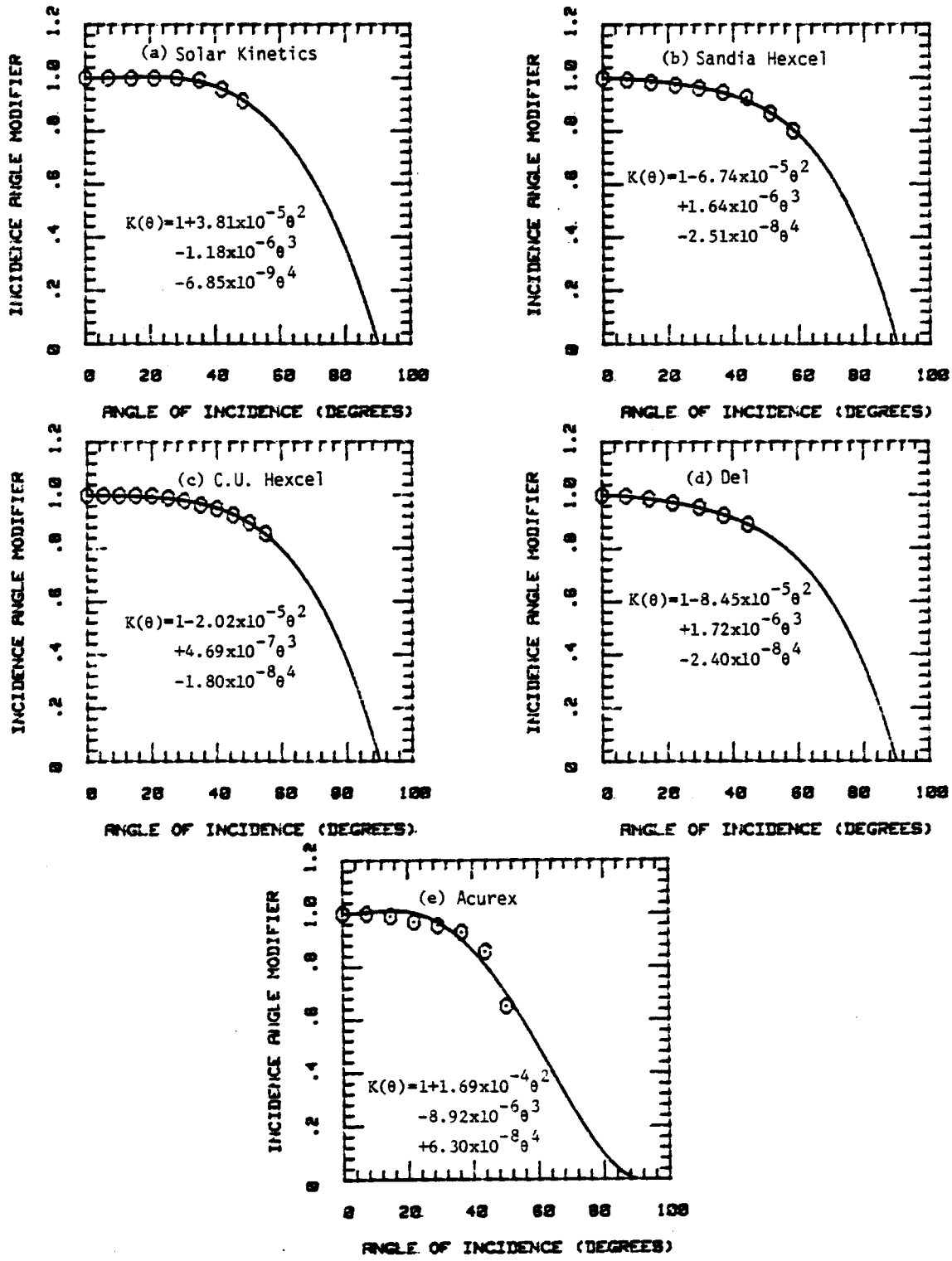

Fig. 4-3(a)-(e). Data Points and Polynomial Fits for Incidence Angle Modifier. For the fits of K(θ) given in these figures, θ must be in degrees.

for $y = K$, Γ, $K\Gamma$, and η_o. The incidence angle is a function of time of day and time of year given by

$$\cos \theta_{EW} = \cos \delta(\cos^2 \omega + \tan^2 \delta)^{1/2}, \quad [5\text{-}5]$$

with δ = solar declination, for collectors with horizontal tracking axes pointing in the east-west direction; and for collectors with horizontal tracking axes pointing in the north-south direction it is given by

$$\cos \theta_{NS} = \cos \delta[\sin^2 \omega + (\cos \lambda \cos \omega + \tan \delta \sin \lambda)^2]^{1/2}, \quad [5\text{-}6]$$

with λ = geographic latitude.

For polar mount the incidence angle equals the declination,

$$\theta_{polar} = \delta, \quad [5\text{-}7]$$

at all times and is so small that the incidence angle modifier can be neglected in most cases.

Strictly speaking, one should calculate $\overline{K\Gamma}$; however, the presentation of the results is greatly simplified with the approximation

$$\overline{\eta}_o = \eta_o(\theta = 0)\,\overline{K\Gamma} = \eta_o(\theta = 0)\,\overline{K}\,\overline{\Gamma}. \quad [5\text{-}8]$$

Therefore, we first investigate (see Table 5-1) the ratio of $\overline{K\Gamma}$ and $\overline{K}\,\overline{\Gamma}$ for three different values of the ratio of the length over focal length, ℓ/f, corresponding to a Hexcel collector operating as a single module, or as two or four modules joined in a row. For this table, as well as the next two tables, the following format has been adopted: all values are calculated for summer solstice, equinox, and winter solstice, for both east-west and north-south mounts, and for each case values are entered for two cutoff times [$t_c = t_s - 1$ hour (top row) and $t_c = t_s - 2$ hours (bottom row)], based on the assumption that the collector operates from t_c hours before noon until t_c hours after noon. The difference between the average of the product and the product of the averages is seen to be small enough to be neglected, since collectors with horizontal tracking axes will usually be installed in long rows.

Therefore, two tables suffice to present the all-day averages. Table 5-2 lists $\overline{\Gamma}$ as a function of ℓ/f, and Table 5-3 lists $\overline{K}$ for each of the collectors that have been tested. Comparison of the entries for different cutoff times t_c indicates variation on the order of 1%. This implies that an all-day average interpolated from these tables is quite acceptable for use in calculations of long term energy delivery.

ACKNOWLEDGMENT

This report was prepared under Contract No. EG-77-C-01-4042, SERI Task 3432.10. The authors thank V. E. Dudley and R. M. Workhoven for valuable discussions and for kindly allowing use of their data before publication.

Table 5-1. Comparison of $\overline{K\Gamma}$ and $\overline{K}\,\overline{\Gamma}$ for Hexcel Collector As Function of Array Length[a]

	$\overline{K}\,\overline{\Gamma}/\overline{K\Gamma}$					
	E-W Axis			N-S Axis		
$\frac{\ell}{f}$	Summer	Equinox	Winter	Summer	Equinox	Winter
6.44	0.987	0.987	0.998	1.000	1.000	0.998
	0.993	0.995	0.999	1.000	1.000	0.999
12.9	0.993	0.993	0.999	1.000	1.000	1.000
	0.996	0.997	0.999	1.000	1.000	1.000
25.7	0.996	0.996	0.999	1.000	1.000	1.000
	0.997	0.998	0.999	1.000	1.000	1.001

[a]Top number represents cutoff time 1 h before sunset; bottom number represents cutoff time 2 h before sunset.

Table 5-2. All-Day Average of End-Loss Factors[a]

$\frac{\ell}{f}$	$\bar{\Gamma}$					
	E-W Axis			N-S Axis		
	Summer	Equinox	Winter	Summer	Equinox	Winter
6.44	0.861	0.872	0.911	0.947	0.899	0.760
	0.880	0.896	0.930	0.967	0.887	0.736
12.9	0.928	0.934	0.952	0.978	0.944	0.873
	0.937	0.944	0.960	0.978	0.938	0.861
25.7	0.961	0.965	0.972	0.984	0.967	0.930
	0.965	0.969	0.975	0.984	0.963	0.924

[a]Top number represents cutoff time 1 h before sunset; bottom number represents cutoff time 2 h before sunset.

Table 5-3. All-Day Average of Incidence Angle Modifier $\bar{K}$ for Various Collectors[a]

Collector Type	$\bar{K}$					
	E-W Axis			N-S Axis		
	Summer	Equinox	Winter	Summer	Equinox	Winter
Del	0.914	0.923	0.960	0.994	0.960	0.843
	0.932	0.946	0.975	0.996	0.953	0.821
Acurex	0.855	0.876	0.954	1.000	0.971	0.683
	0.890	0.921	0.988	1.000	0.963	0.627
Solar Kinetics	0.946	0.954	0.990	1.000	0.997	0.891
	0.964	0.977	1.000	1.000	0.996	0.866
Hexcel, Sandia	0.927	0.935	0.969	0.995	0.970	0.868
	0.944	0.957	0.981	0.997	0.965	0.847
Hexcel, SERI	0.938	0.945	0.980	0.998	0.983	0.883
	0.955	0.968	0.990	0.999	0.980	0.861

[a]Top number represents cutoff time 1 h before sunset; bottom number represents cutoff time 2 h before sunset.

NOMENCLATURE

f	Focal length
F'	Factor in Hottel-Whillier-Bliss equation which accounts for difference between fluid temperature and absorber surface temperature
I	Insolation on aperture = $I_b \cos\theta$ (W/m^2)
I_b	Beam irradiance as measured by pyrheliometer (W/m^2)
$K(\theta)$	$\eta_o(\theta)/\eta_o(\theta = 0)$ incidence angle modifier for collectors without end loss
$\bar{K}$	All-day average incidence angle modifier
ℓ	Length of collectors
r	Amount by which receiver extends beyond aperture
t	Time of day (measured from solar noon)
t_c	Cutoff time
t_s	Sunset time
T_a	Ambient temperature
T_f	Mean fluid temperature = $(T_{in}+T_{out})/2$
T_{in}	Inlet fluid temperature
T_{out}	Outlet fluid temperature
ΔT	$T_f - T_a$
U	Heat loss coefficient or U_2 value, relative to aperture area (W/m^2 °C)
α	Absorptance of receiver
γ	Intercept factor = fraction of rays incident on aperture which reach receiver if collector has no end loss
$\Gamma(\theta)$	End-loss factor

$\bar{\Gamma}$	All-day average of Γ
δ	Solar declination
$\eta(\theta)$	Collector efficiency at incidence angle θ
$\eta_o(\theta)$	Optical efficiency = $(\rho\tau\alpha)\ \gamma$
$\bar{\eta}_o$	All-day average of η_o
θ	Incidence angle on collector, measured along trough axis from collector normal
λ	Geographic latitude
ρ	Reflectance
$(\rho\tau\alpha)$	Effective reflectance-transmittance-absorptance product
τ	Transmittance
ω	Hour angle = $2\pi t/T$ (T = 24 h)
ω_c	Cutoff hour angle = $2\pi t_c/T$
ω_s	Sunset hour angle = $2\pi t_s/T$

REFERENCES

(1) Hill, J.E.; Streed, E. R. "A Method of Testing for Rating Solar Collectors Based on Thermal Performance." Solar Energy. Vol. 18: p.421; 1976.

(2) Simon, F. F. "Flat Plate Solar Collector Performance Evaluation with a Solar Simulator as a Basis for Collector Selection and Performance Prediction." Solar Energy. Vol. 18: p.451; 1976.

(3) Tabor, H. "Testing of Solar Collectors." Solar Energy. Vol. 20: p.293; 1978.

(4) American Society of Heating, Refrigeration, and Air-Conditioning Engineers, Inc. ASHRAE Standard, Method of Testing to Determine The Thermal Performance of Solar Collectors. New York, NY: ASHRAE; 1978.

(5) Dudley, V. E.; Workhoven, R. M. Summary Report: Concentrating Solar Collector Test Results Collector Module Test Facility. Albuquerque, NM: Sandia Labs.; 1978; SAND 78-0815.

Dudley, V. E.; Workhoven, R. M. Summary Report: Concentrating Solar Collector Test Results Collector Module Test Facility, January-December 1978. Albuquerque, NM: Sandia Labs; 1979; SAND 78-0977 (1979).

Also reports on individual collectors: for Hexcel collector, SAND 78-0381 (1978); for Del collector, SAND 79-0515 (1979).

(6) Duffie, J. A.; Beckman, W. A. Solar Energy Thermal Processes. New York: John Wiley and Sons; 1974.

(7) Kreith, F.; Kreider, J. F. Principles of Solar Engineering. New York: McGraw-Hill Book Co.; 1978.

(8) Bendt, P.; Rabl, A.; Reed, K. A.; Gaul, H. W. Optical Analysis and Optimization of Line Focus Solar Collectors. Golden, CO: Solar Energy Research Institute; SERI/TR-34-092. To be published.

(9) Dudley, V. E.; Workhoven, R. M. Personal communication.

(10) Bendt, P.; Gaul, H. W.; Rabl, A. How to Measure The Optical Quality of Concentrating Collectors Without Laser Ray Tracing. Golden, CO: Solar Energy Research Institute; SERI/TR 34-251. To be published.

(11) Collares-Pereira, M.; Rabl, A. Simple Procedure for Predicting Long-term Average Performance of Nonconcentrating and of Concentrating Solar Collectors. Argonne, IL: Argonne National Lab.; ANL-78-67. To be published in Solar Energy.

(12) Collares-Pereira, M.; Rabl, A. "The Average Distribution of Solar Radiation: Correlations between Diffuse and Hemispherical and between Daily and Hourly Insolation Values." Solar Energy. Vol. 22: p.155; 1979.